Assessment of Small Damage by Direct Modal Strain Measurements

G. De Roeck(✉), E. Reynders, and D. Anastasopoulos

Department of Civil Engineering,
KU Leuven, Kasteelpark Arenberg 40, 3001 Leuven, Belgium
guido.deroeck@kuleuven.be

Abstract. Vibration based Structural Health Monitoring was and is still a hot topic in research. Much progress has been made both from the theoretical as well as the practical side. Vibration-based SHM traditionally makes use of uniaxial/triaxial accelerometers or velocity meters. Also sometimes inclinometers are installed. Recent trends in SHM are the use of high-rate GPS receivers [1], wave propagation-based piezoelectric ceramic sensing technology and optical fiber sensors for dynamic strain and temperature measurements [2].

A particular challenge for structural health assessment is the discovery of small local damage. It is well known that for small damages, the changes in natural frequencies remain very low. Moreover, they are considerably influenced by environmental conditions (mainly temperature) [3], which influence has to be eliminated on beforehand [4, 5]. Also modal displacements are rather insensitive to small stiffness perturbations. On the contrary, modal strains (or curvatures) are very receptive to small stiffness changes. Additionally, they immediately spot the damage location. Some authors have tried to derive curvatures from modal displacements but this procedure is very prone to even slight measurement and/or identification errors. Therefore, the key issue is the direct measurement of (modal) strains. However, the development of a distributed strain sensor network able to cope with the very low strain intensities during ambient excitation is still a challenge. In this paper by recent experiments on steel and concrete beams the extreme accuracy of dynamic measurements with optical FBG strain sensors is demonstrated.

Another possibility to obtain precise modal strains would be the development of a transducer that amplifies the strains. In a recent research project, by using Topology Optimization [6], a transducer was developed that measures differential axial displacements over a sufficient long distance and at the same time is upscaling the strains. Results obtained with this transducer are reported.

In this context, a new challenge for Optimal Sensor Placement [7] is to deal with different sensor types, e.g. displacement transducers, accelerometers and strain sensors.

For localization and quantification of damage, the most powerful method is FE-model updating based on minimizing differences between measured and calculated modal parameters [8]. The addition of modal strains to the objective function of the minimization problem will improve the damage identification process.

Keywords: Modal analysis · Modal strains · Damage assessment · Structural health monitoring · Optical strain fibers

J.P. Conte et al. (eds.), *Experimental Vibration Analysis for Civil Structures*,
Lecture Notes in Civil Engineering 5, https://doi.org/10.1007/978-3-319-67443-8_1

1 Introduction

Vibration-based structural health monitoring (SHM) is based on the principle that modal parameters of a structure are like a signature of structural behaviour. Output-only or operational modal analysis (OMA) became very popular as no artificial vibration source is needed which is anyhow impossible in many cases. Powerful time domain system identification algorithms like Stochastic Subspace Iteration (SSI) have replaced the obsolete "peak-picking" method [9, 10].

Vibration-based SHM traditionally makes use of uniaxial/triaxial accelerometers or velocity meters. Also sometimes inclinometers are installed. Recent trends in SHM are the use of high-rate GPS receivers [1], wave propagation-based piezoelectric ceramic (PZT) sensing technology and optical fiber sensors (OFS) for dynamic strain and temperature measurements [2].

Because of the omission of cables, wireless networks (WNs) have a lot of evident advantages, like the ease of system setup, the largely reduced installation time, the possibility of local data processing, data interpretation and anomaly detection. In a recent project a wireless measurement with high time-synchronization accuracy was developed [11]. Spatial jitter was reduced to 125 ns, far below the 120 μs required for high-precision acquisition systems and much better than the 10-μs current solutions, without adding complexity. Moreover, the system is scalable to a large number of nodes to allow for dense sensor coverage of real-world structures.

In most of modal testing campaigns, there are more degrees-of-freedom (DOFs) to be measured than sensors available. The whole measurement grid then needs to be covered in several phases by different measurement setups. A number of reference locations are then selected and transducers at these points are often kept fixed in all setups. The ideal location for a reference sensor is a position where all modes have relatively large modal amplitudes. However, there exists no guidelines or general principles for evaluating whether a chosen number of reference sensors leads to sufficiently accurate mode shape estimates. In practice, even when measuring large structures, often a very limited number of reference sensors is allocated. The other transducers are roved in successive setups, hence these transducers are often termed `roving' sensors, so that by the end of the last setup, vibration responses at all grid points will have been recorded. So for any measurement campaign, the following questions have to be answered: (i) the location of the reference sensors, (ii) their number, (iii) the location of the roving sensors in the different setups. Answers can be given by applying Optimal sensor location (OSL) approaches. In [7] their practical applicability has been illustrated on a large-scale operational modal test of a five-span steel truss railway bridge. The measurement layout was designed according to intuitive reasoning, based on the modal results of a preliminary Finite Element analysis. Afterwards, this test design has been reviewed using OSL. A new challenge is to deal with different sensor types, e.g. displacement transducers, accelerometers and strain sensors.

Results can be used for calibration of numerical FE-models inherently containing uncertainties especially related to boundary conditions, joint stiffnesses, structural contribution of non-bearing parts, material parameters, damping, …

Subsequently, properly calibrated FE-models can be used to derive from response measurements the actual excitation like moving loads on road or railway bridges and wind forces on tall structures. Moreover, these models can be used to obtain from the response measurements in a limited number of sensors information in otherwise difficult to assess points, like strains close to weldings or forces in bolts [12].

Other interesting applications relate to the follow-up of critical phases during erection of constructions.

Moreover, changes in modal parameters (i.e. natural frequencies, damping ratios, mode shapes and modal strains) can be used as features to detect and to identify damage. Compared to other approaches for structural damage identification, vibration-based damage identification has the advantages of (1) being nondestructive, (2) being able to identify damage that is invisible at the surface, (3) being 'global' because no a priori location of the damage needs to be assumed as opposed to local methods such as ultrasonic testing. A good overview of recent trends is given in [13].

Unfortunately, modal parameters are not only sensitive to damage, but also to changing environmental conditions such as temperature variations, and moreover, their estimation from vibration response data is also prone to experimental errors. This is well known for natural frequencies but less observed and understood for mode shapes and modal strains. Challenge is to eliminate the environmental influences by prediction models that just rely on estimated modal properties (i.e. output-only models [4]) or on the measured environment as input and the estimated modal parameters as output (i.e. input-output models [5]). These models are trained by using data gathered in undamaged condition.

2 Small Local Damage

2.1 Background

A particular challenge for structural health assessment is the discovery of small local damage. Not only natural frequencies and mode shapes will hardly be affected but also its influence hidden in the uncertainty blur. Therefore, the development of a distributed strain sensor network able to cope with the very low strain intensities during ambient excitation is a challenge. Optical fiber sensors with Bragg grating technology permanently attached to the structure could be a good choice in this respect. Interrogation units are still quite expensive but can be coupled and uncoupled when adopting a periodic monitoring maintenance strategy. An additional advantage of the measured strain field is that it can be directly related to the stress field. Such a system will also be able to measure quasi-static deformation as occurs in case of shrinkage, creep, thermal expansion and very slowly applied dynamic loads. The idea of directly measuring accurate strains is explored in the next sections.

2.2 Upscaling Strain Transducer

During ambient excitation strains are very small so extracting modal strains is rather cumbersome. Moreover, in concrete structures when mean strains are measured over a long enough stretch, the classical Bernoulli assumption that plane sections remain plane

is still reasonably well fulfilled. This also implies that (modal) curvatures can be used for damage assessment.

Therefore a transducer that measures differential axial displacements over a sufficient long distance and at the same time amplifies the strains would be of great benefit. In a recent research project such transducer was developed by using Topology Optimization [14]. The transducer is connected by bolts to the test structure (Fig. 2: points 1 and 2). The actual strain is the one between the two bolts. The goal of the Topology Optimization is to amplify the strain occurring between points A and B (Fig. 1), which is measured by a Bragg grating on an optical fiber between these two points.

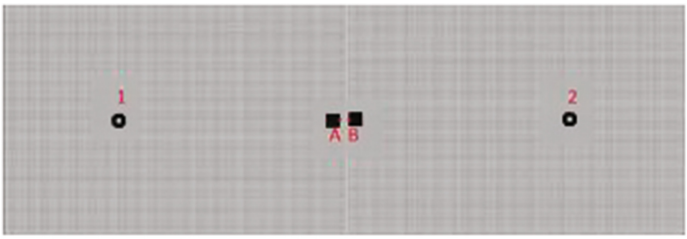

Fig. 1. Grid used in the topology optimization.

In Topology Optimization, a design is obtained by optimizing the distribution of a certain amount of material in the design domain. This design domain (grid) is displayed in Fig. 2. Note that some elements of this design domain are filled with material in advance. This due to the way the transducer and optical fiber will be mounted. The objective of the optimization is to minimize the horizontal displacement at the fixation point of the fiber, in case a positive horizontal force is applied at the fixation bolt of the transducer. This obtained by defining a minimum compliance optimization function as described in Wang (2011) [19]:

$$\min_{x} c(\boldsymbol{x})$$

$$\textit{subject to} : \boldsymbol{KU} = \boldsymbol{F}; \quad \frac{V}{V_0} \leq f_v; \quad 0 \leq x_e \leq 1 \tag{1}$$

In this equation, **x** is the vector with the element densities x_e, ranging from 0 (void) to 1 (solid). These element densities will be altered to obtain an optimal objective value c. **K** is the global stiffness matrix, **U** is the global displacement vector containing the displacements in all degrees of freedom and **F** is the global force vector. V is the material volume and V_0 is the total volume of the design domain. The ratio of these parameters must be smaller than a prescribed volume fraction f_v. This volume constraint is applied to this optimization, ensuring the total amount of material remains below a certain amount. Through calibration a volume constraint of 50% was selected, as a higher volume would not result in a higher objective value but would have a negative influence on the natural frequencies of the transducer.

The optimum of the objective function is calculated using the Method of Moving Asymptotes [6]. This algorithm will iteratively calculate the optimum. Convergence will be assumed when a change in material distribution of less than 5% occurs. This standard optimization approach results in one node hinges and bending in the optical fiber. To obtain a more robust design, extra constraints are applied. The first constraints ensured a local length scale control, preventing one node hinges. Another constraint was added, ensuring the mounting platforms of the optical fiber will not rotate, preventing bending of the fiber. This algorithm will iteratively calculate the optimum. Convergence will be assumed when a change in material distribution of less than 5% occurs.

The result of the optimization is shown in Fig. 2. A strain amplification by a factor 120 can theoretically be obtained.

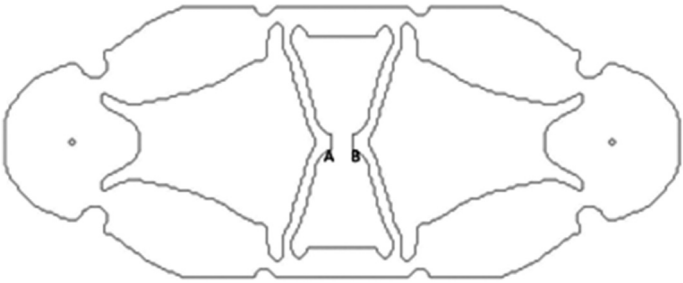

Fig. 2. Strain transducer from Topology Optimization.

Figure 3 shows a displacement plot by ANSYS for the right half of the sensor. A compression between 1 and 2 results in an elongation of AB. A prototype of this

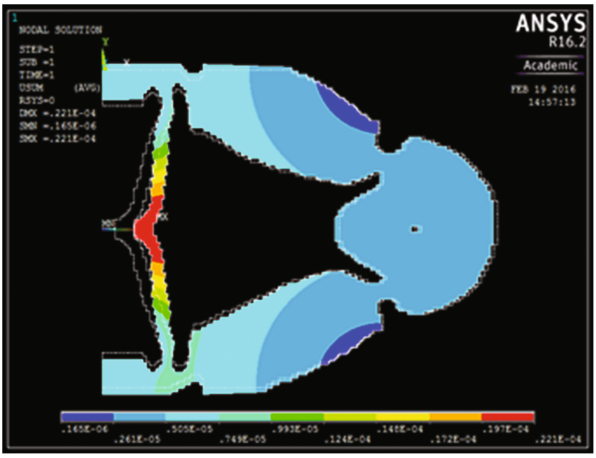

Fig. 3. Displacement plot.

sensor has been produced by laser cutting and its upscaling factor tested in the laboratory [14].

2.3 Strain Optical Fiber Network

To demonstrate the high accuracy that can be obtained from optical fiber strain sensors, an extensive experimental modal analysis test has been performed on a steel I-beam IPE 100 (Fig. 4) at the Structural Mechanics Laboratory of KU Leuven [15, 16]. The length of the beam is 3.0 m and steel plates are welded at its ends. The boundary conditions are set to approximate free-free conditions. For that purpose, the beam was

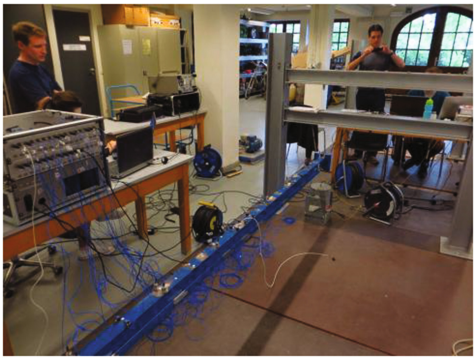

Fig. 4. Instrumented steel beam.

suspended on flexible springs. The beam was excited through a shaker located at the left end (Fig. 5) with various force amplitudes (2.3–13.5 N) and excitation signals (pure random, swept sign, periodic random) from [0:200] Hz and from [0:500] Hz. The low forces produce strain RMS values below one micro-strain.

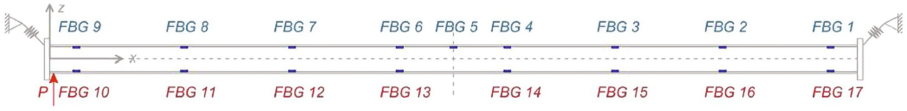

Fig. 5. FBGs setup - front view.

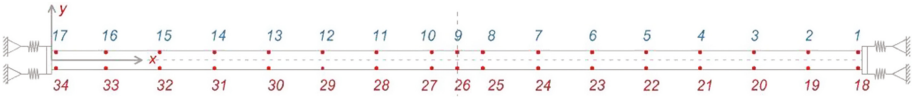

Fig. 6. Accelerometers setup - top view.

The beam was instrumented with a chain of multiplexed Bragg Grating (FBG) strain sensors glued at the top and the bottom flange of the beam (Fig. 5) and accelerometers (Fig. 6). The sampling frequency was f_s = 20000 Hz for the accelerometers and f_s = 950 Hz for the FBGs.

FBG based sensing relies on tracking the Bragg peak wavelength as it shifts with a change in the measured peak. Recently a fast and accurate peak detection algorithm has been recently proposed [17]. The fast phase-correlation (FPC) algorithm determines the wavelength shift from the phase shift between the undisturbed FBG spectrum and the perturbed spectrum.

Three modal analyses were performed by applying the Matlab toolbox MACEC [18] with two algorithms, SSI-cov and CSI [10]: (1) using FBG strain data; (2) using accelerometer data; (3) using both data. In the latter case, the accelerometer data were down-sampled at 950 Hz.

In the interval [0:200] Hz 2 bending modes and 3 torsional modes could be identified. An excellent correspondence with FE calculated modal properties is observed [16]. Moreover, the obtained modal characteristics from the combined modal analysis show a high consistency with the ones obtained from the separate analyses. The differences in modal displacements are less than 5%. The combined analysis, using data from both FBG strain sensors and accelerometers, allows to obtain mass normalized modal strains. Mass normalization is possible because acceleration was measured at the same location and direction as the applied force. Figure 7 shows the

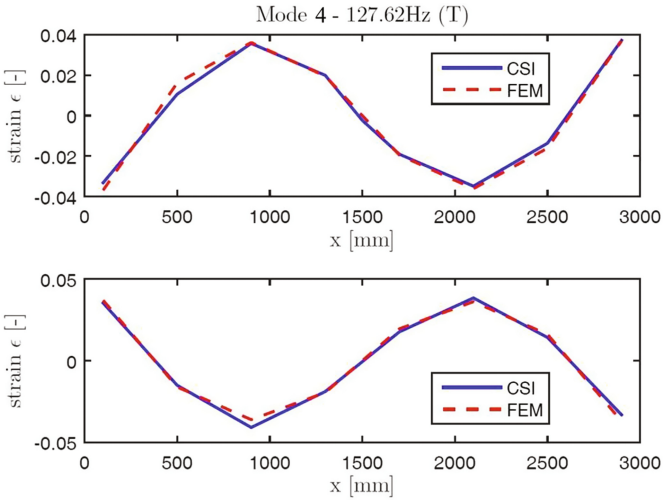

Fig. 7. Normalized modal strains of the third torsional mode T3.

comparison between calculated and measured mass normalized strains. Remarkable is the excellent agreement, taken into account the very low strain levels and the longitudinal orientation of the FBG strain fibers. They sense the torsional modes because of the restrained warping effect.

2.4 Damage Identification by Modal Strains

In a very recent experiment the ability of modal strains to identify more accurately structural damage in reinforced concrete beams is investigated. In order to comply with the Bernoulli assumption for beams, mean strains have to be measured over a suffi-

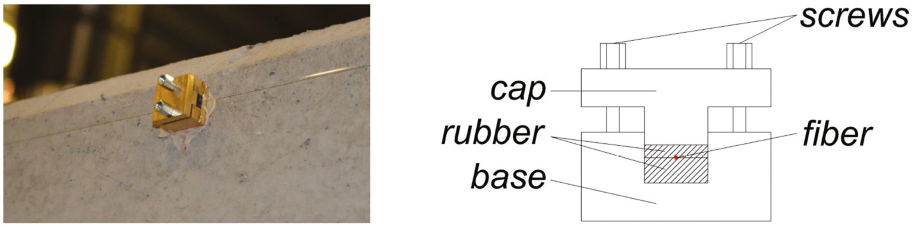

Fig. 8. Connector system for optical strain fiber.

ciently long length (e.g. typically one or two crack distances). Small measurement lengths will show a clear discontinuous behavior, depending on the location of the strain sensor: above a crack or between cracks.

A connector (Fig. 8) has been developed to clamp an optical glass fiber containing

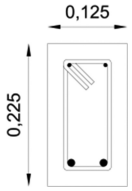

Fig. 9. Beam cross section.

several Bragg gratings at discrete points with proper spacing.

The experiment is aiming to identify the dynamic characteristics of a reinforced concrete beam at increasing damage levels. The beam has a length of 1.7 m and a rectangular cross section with dimensions 125 × 225 mm (Fig. 9). Steel reinforcement consists of 2 bars of 12 mm diameter at the tensile side and 2 bars of 8 mm at the compression side.

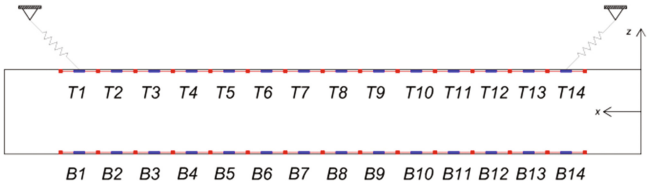

Fig. 10. FBG sensors setup - front view.

Shear reinforcement is by stirrups of 6 mm diameter. Concrete cover of these stirrups is 25 mm.

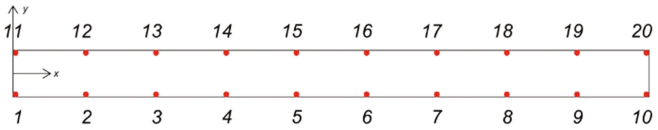

Fig. 11. Accelerometers setup - top view.

Two chains of multiplexed FBG strain sensors were attached: one on the front side at the bottom and on the back side at the top (Fig. 10). Each chain contains 14 FBG

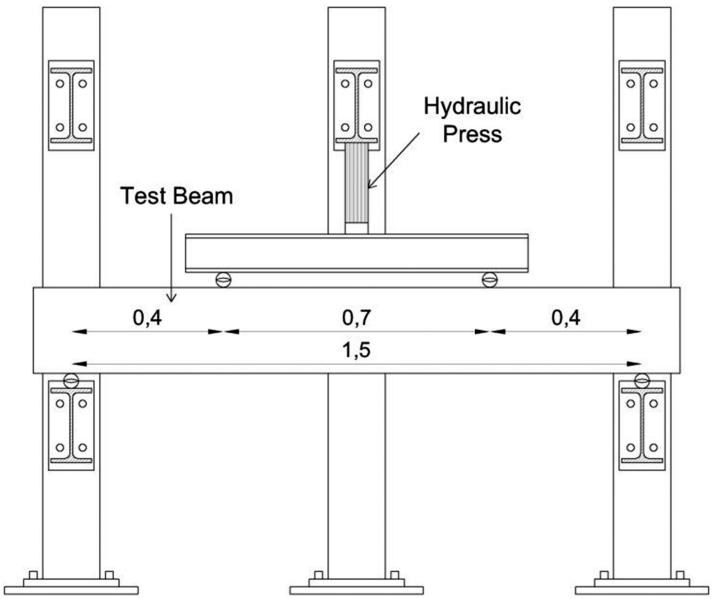

Fig. 12. Four point bending static test setup.

sensors which measure the average strain along a length of 100 mm. The chains measure the strains of the beam at a distance of about 1 cm from its edges.

At the top side of the beam 20 accelerometers were installed (Fig. 11). The distance between the accelerometers was about 20 cm.

Prior to the dynamic tests, damage is induced by static loads in a four point bending configuration (Fig. 12).

After each static test producing progressive damage, the beam is suspended from flexible springs, approaching dynamic free-free boundary conditions, to perform a modal identification. Dynamic response is provoked by hammer impacts and by a

shaker, exciting both the bending and the torsion modes. Input signal to the shaker is a sine sweep. The sampling frequency of the FBG strain acquisition system (FAZT I4) is f_s = 1000 Hz and 10000 Hz for the acceleration acquisition system (NI PXI-1050 chassis with NI PXI-4472B modules).

In the initial state, by using the acceleration data in MACEC, three vertical bending

Table 1. Natural frequencies

Mode	Type	f (Hz) ANSYS	f (Hz) measured	Difference (%)
1	L1	172	168	2.5
2	B1	304	301	1.3
3	L2	460		
4	T1	589	590	−0.2
5	B2	767	761	0.7
6	L3	865		
7	A1	1175		
8	T2	1179	1184	−0.4
9	B3	1356	1371	−1.1
10	L4	1360		
11	T3	1771	1766	0.3

modes (B1, B2, B3) and three torsional modes (T1, T2, T3) are identified (Table 1). When applying system identification to the strain data, only one lateral bending mode (L1) and one vertical bending mode (B1) could be extracted due to the limited sampling frequency of the FBG strain acquisition system. No axial modes (A) are found. In Table 1 also a comparison is made with a FE model (ANSYS) consisting of solid elements for the concrete and truss elements for the reinforcement.

Table 2 gives a view of the corresponding experimental mode shapes.

Damage is applied at different static loads (Fig. 12) till failure. Dynamic tests are performed after each unloading and change of boundary conditions to free-free, by attaching the beam to flexible springs. The extensive dataset is currently analyzed. Some preliminary results obtained after applying a static load P of 80 kN are presented. This load exceeds the crack load (about 30 kN). Table 5 resumes the frequency shifts. Despite the clear decrease of natural frequencies, the changes in mass normalized mode shapes are rather small, as shown in Table 3 for the first bending mode B1 and the third bending mode B3. The changes for the higher mode B3 are more pronounced, but still small.

The simultaneous measurement of accelerations (at the location of the applied load) and strains also allows to obtain mass normalized modal strains.

Table 4 shows for mode B1 the mass normalized modal strains at the top (left column) and at the bottom (right column). Results are given at initial undamaged state and at P equal to 80 kN. The initial modal strains, measured over a length of 10 cm) show a very good correspondence with the mass normalized strains from the FE model.

For the damaged beam the modal strains are more irregular. One of the reasons could be the short measurement length (10 cm) compared to the mean crack spacing, which is about 9 cm. Integrating over a longer length (by summing up over several

Table 2. Mode shapes

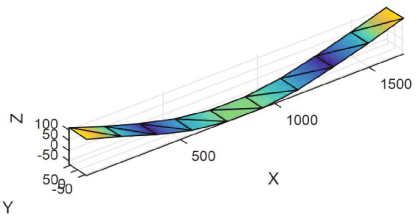	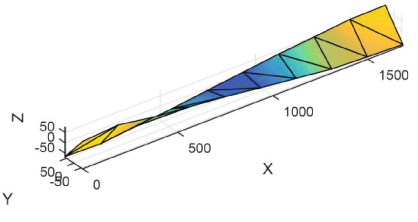
Mode shape B1 – 301 Hz	Mode shape T1 – 590 Hz
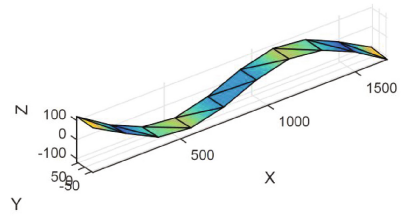	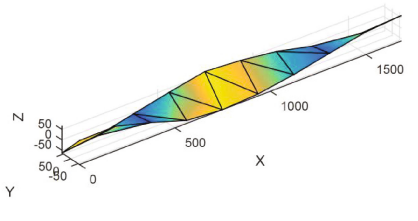
Mode shape B2 – 761 Hz	Mode shape T2 – 1184 Hz
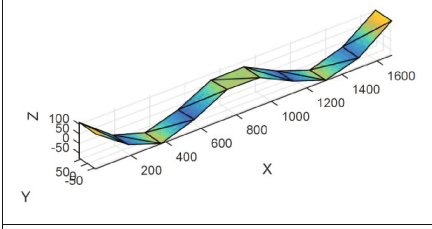	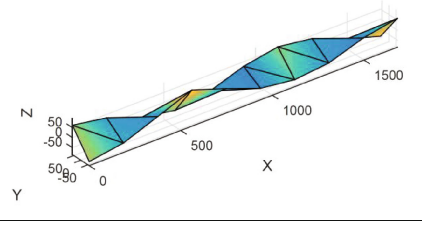
Mode shape B3 – 1371 Hz	Mode shape T3 – 1766 Hz

Table 3. Mass normalized mode shapes B1 and B3, before (blue) and after damage (red).

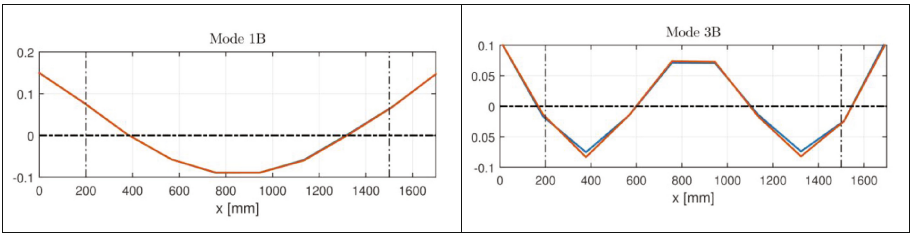

Table 4. Changes in mass normalized modal strains of mode B1: measured versus FE simulated

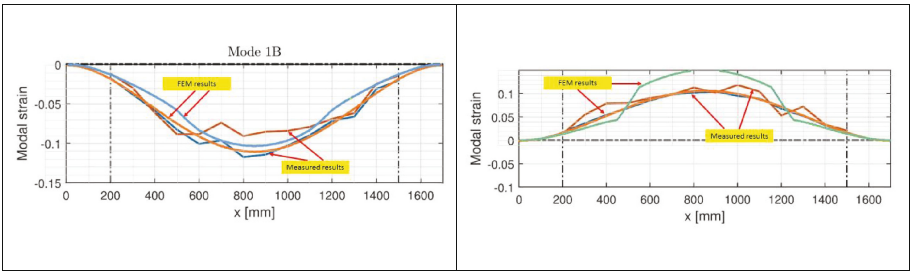

Table 5. Change of natural frequencies (at P = 80 kN)

	Acceleration data - CSI		
	Undamaged beam	Damaged beam (80KN)	Percentile difference
Mode	frequency (Hz)	frequency (Hz)	%
B1	300.50	248.20	-17.4
T1	590.30	501.50	-15.0
B2	761.30	629.30	-17.3
T2	1183.70	1019.10	-13.9
B3	1371.40	1132.70	-17.4
T3	1765.90	1564.00	-11.4
	Strain data - SSI-cov		
	Undamaged beam	Damaged beam (80KN)	Percentile difference
Mode	frequency (Hz)	frequency (Hz)	%
L1	168.00	139.20	-17.1
B1	300.60	249.70	-16.9
	Combined data - CSI		
	Undamaged beam	Damaged beam (80KN)	Percentile difference
Mode	frequency (Hz)	frequency (Hz)	%
B1	300.60	249.70	-16.9

sensors) will result in a smoother behavior. Comparison is also made with an approximate FE model in which the E-modulus of the tensile zone of the central, most damaged part of the beam (zone of 0.7 m in Fig. 12) is reduced in a way that the calculated natural frequencies are close to the measured values of Table 5. From this simulation it can be concluded that the observed changes in mass normalized modal strains go in the right direction: a reduction at the top (compression) side and an increase at the tensile (bottom side). However, quantitatively there are important differences that need further investigation.

Much more information will be available when the measured static and dynamic results of the different loading steps will be treated. The strain results will be opposed to the observed crack patterns at successive loads. The suitability of the designed clamping system will be investigated, e.g. by carefully analyzing the elastic strains at low load levels.

3 Conclusions

The ability to discover small damage by vibration monitoring is driven by the development of new sensor types, especially those that measure very low dynamic strains, and their application at proper locations by using optimal sensor location algorithms. A laboratory test shows that accurate mode shapes and modal strains can be obtained from acceleration and FBG measurements, even at very low excitation levels. The very low strain levels during ambient excitation can be amplified by a proper transducer design. For reinforced (and prestressed) concrete structures a system has been developed that allows to measure small modal strains (and curvatures) over a length which is in correspondence with classical theory for (cracked) reinforced beams.

Acknowledgments. The research presented in this paper has been performed within the framework of the project G099014N "Identification and modeling of structural damage", funded by the Research Foundation Flanders (FWO), Belgium. Their financial support is gratefully acknowledged.

References

1. Yi, T.H., Li, H.N., Gu, M.: Experimental assessment of high-rate GPS receivers for deformation monitoring of bridge. Measurement **46**(1), 420–432 (2013)
2. Lopez-Higuera, J.M., Cobo, L.R., Incera, A.Q., Cobo, A.: Fiber optic sensors in structural health monitoring. J. Lightwave Technol. **29**(4), 587–608 (2011)
3. Deraemaeker, A., Reynders, E., De Roeck, G., Kullaa, J.: Vibration based structural health monitoring using output-only measurements under changing environment. Mech. Syst. Signal Process. **22**(1), 34–56 (2008)
4. Reynders, E., Wursten, G., De Roeck, G.: Output-only structural health monitoring in changing environmental conditions by means of nonlinear system identification. Struct. Health Monit. **13**(1), 82–93 (2014)
5. Reynders, E., De Roeck, G.: Robust structural health monitoring in changing environmental conditions with uncertain data. In: Proceedings of the 11th International Conference on Structural Safety and Reliability, ICOSSAR, 2003, New York, NY, USA, 16–20 June 2013 (2013)
6. Bendsoe, M.P., Sigmund, O.: Topology Optimization: Theory Methods and Applications. Springer, New York (2003)
7. Bui, T.T., Reynders E., Lombaert G., De Roeck, G.: Ambient vibration testing of a large truss bridge with optimal sensor placement. In: Gao, G., Tutumluer, E., Chen, Y. (eds.) Recent Advances in Environmental Vibration; Proceedings of the 6th International Symposium on Environmental Vibration. China Scientific Book Services (2013)

8. Teughels, A., De Roeck, G.: Damage detection and parameter identification by finite element model updating. Arch. Comput. Methods Eng. **12**(2), 123–164 (2005)
9. Peeters, B., De Roeck, G.: Reference-based stochastic subspace identification for output-only modal analysis. Mech. Syst. Signal Process. **13**(5), 855–878 (1999)
10. Reynders, E., De Roeck, G.: Reference-based combined deterministic-stochastic subspace identification for experimental and operational modal analysis. Mech. Syst. Signal Process. **22**(3), 617–637 (2008)
11. Araujo, A., García-Palacios, J., Blesa, J., Tirado, F., Romero, E., Samartín, A., Nieto-Taladriz, O.: Wireless measurement system for structural health monitoring with high time-synchronization accuracy. IEEE Trans. Instrum. Meas. **61**(3), 801–810 (2012)
12. Lourens, E., Papadimitriou, C., Gillijns, S., Reynders, E., De Roeck, G., Lombaert, G.: Joint input-response estimation for structural systems based on reduced-order models and vibration data from a limited number of sensors. Mech. Syst. Signal Process. **29**, 310–327 (2012)
13. Cunha, A., Caetano, E., Magalhães, F., Moutinho, C.: Recent perspectives in dynamic testing and monitoring of bridges. Struct. Control Health Monit. **20**(6), 853–877 (2013)
14. Jonckers, T.: Development of High-accuracy Strain Sensors using Topology Optimization, MSc Thesis, KU Leuven (2016)
15. Anastasopoulos, D., Moretti, P., Geernaert, T., De Pauw, B., Nawrot, U., De Roeck, G., Berghmans, F., Reynders, E.: Modal strain identification from low-amplitude FBG data using an improved wavelength detection algorithm. In: Bakker, J., Frangopol, D.M., van Breugel, K. (eds.) Proceedings of the 5th International Symposium on Life-Cycle Civil Engineering, IALCCE 2016, pp. 319–326. Delft, The Netherlands, Taylor & Francis (2016)
16. Anastasopoulos, D., Moretti, P., Geernaert, T., De Pauw, B., Nawrot, U., De Roeck, G., Berghmans, F., Reynders, E.: Identification of modal strains using sub-microstrain FBG data and a novel wavelength-shift detection algorithm. Mech. Syst. Signal Process. **86**, 58–74 (2017)
17. Lamberti, A., Vanlanduit, S., De Pauw, B., Berghmans, F.: A novel fast phase correlation algorithm for peak wavelength detection of fiber bragg grating sensors. Opt. Express **22**(6), 7099–7112 (2014)
18. Reynders, E., Schevenels, M., De Roeck, G.: MACEC 3.3: a Matlab toolbox for experimental and operational modal analysis, BWM-2014-06, KU Leuven, internal report (2014)
19. Wang, F., Lazarov, B.S., Sigmund, O.: On projection methods, convergence and robust formulations in topology optimization. Struct. Multidisciplinary Optim. **43**, 767–784 (2011)